

Cingulate to septal circuitry facilitates the preference to affiliate with large peer groups

Highlights

- Spiny mice, but not C57BL/6J mice, exhibit affiliative-peer-group preferences
- The ACC-LS circuit is necessary for group investigation preferences in spiny mice
- Inhibition of the ACC-LS reverses affiliative group preferences in male spiny mice
- The ACC-LS circuit does not modulate nonsocial group size preferences in spiny mice

Authors

Brandon A. Fricker, Malavika Murugan, Ashley W. Seifert, Aubrey M. Kelly

Correspondence

aubrey.kelly@emory.edu

In brief

Fricker et al. demonstrate that the ACC-LS circuit is necessary for peer group size preferences in communally breeding male and female spiny mice. These findings show that the ACC-LS circuit is an integral mediator of peer group affiliation responses that are likely critical for the formation and possibly the cohesion of complex mammalian societies.

Article

Cingulate to septal circuitry facilitates the preference to affiliate with large peer groups

Brandon A. Fricker,¹ Malavika Murugan,² Ashley W. Seifert,³ and Aubrey M. Kelly^{1,4,5,*}

¹Department of Psychology, Emory University, 36 Eagle Row, Atlanta, GA 30322, USA

²Department of Biology, Emory University, 1510 Clifton Road NE, Atlanta, GA 30322, USA

³Department of Biology, University of Kentucky, 211 Thomas Hunt Morgan Building, Lexington, KY 40506, USA

⁴X (formerly Twitter): @AubreyMKelly

⁵Lead contact

*Correspondence: aubrey.kelly@emory.edu

<https://doi.org/10.1016/j.cub.2024.08.019>

SUMMARY

Despite the prevalence of large-group living across the animal kingdom, no studies have examined the neural mechanisms that make group living possible. Spiny mice, *Acomys*, have evolved to live in large groups and exhibit a preference to affiliate with large over small groups. Here, we determine the neural circuitry that facilitates the drive to affiliate with large groups. We first identify an anterior cingulate cortex (ACC) to lateral septum (LS) circuit that is more responsive to large than small groups of novel same-sex peers. Using chemogenetics, we then demonstrate that this circuit is necessary for both male and female group investigation preferences but only males' preference to affiliate with larger peer groups. Furthermore, inhibition of the ACC-LS circuit specifically impairs social, but not nonsocial, affiliative grouping preferences. These findings reveal a key circuit for the regulation of mammalian peer group affiliation.

INTRODUCTION

For many species, including humans, environmental pressures have led to a high degree of sociality associated with living in large groups. Indeed, living in large groups provides species with numerous advantages, such as collective traveling,^{1,2} reduced predation,^{3–5} enhanced offspring survival,^{6–8} and more effective homeostatic regulation,^{9,10} and thus has evolved numerous times across taxa, including in insect,^{11,12} avian,^{13,14} and mammalian species.^{15–17} Identifying neural mechanisms that drive mammals to group can be difficult due to a lack of lab-tractable organisms that naturally evolved to live in large groups. Field studies have found that spiny mice of the genus *Acomys* live in the Israeli desert in mixed-sex groups ranging from 12 to 46, with several *Acomys* species coexisting on the same home range,¹⁸ whereas field studies in food-abundant habitats have documented much higher densities.¹⁹ In the lab, both male and female *Acomys cahirinus* (now known to be *Acomys dimidiatus*) are successfully housed in same-sex groups of 30 of mixed genetic relation,²⁰ allowing for the unique opportunity to study non-reproductive behaviors in peer groups of both sexes. Unlike other lab-tractable mammals, spiny mice exhibit little aggression and are highly prosocial with conspecifics, regardless of age, novelty, familiarity, genetic relation, or reproductive/non-reproductive context.^{15,21,22} Further, spiny mice exhibit a preference to affiliate with larger groups over smaller ones^{15,22} and readily accept newcomers into established groups.²³ Spiny mice are thus an ideal model for inquiries about brain adaptations that arose to support the fundamental building blocks of prosociality and grouping behaviors that are

precursors to even more complex social behaviors, including cooperation.

The lateral septum (LS) is a burgeoning hub for numerous social behaviors and may therefore be important for aspects of group living. Historically, the LS was known for “septal rage,”^{24–27} with recent studies continuing to demonstrate a role for the LS in facilitating aggression in rats and mice.^{28,29} However, a more dynamic role of the LS has been emerging due to recent findings that the LS modulates social recognition in rats^{30,31} and spiny mice²¹ and promotes affiliative behaviors in voles and birds.^{13,32,33} The LS receives inputs from several subcortical regions, positioning the LS to integrate sensory information critical for getting along with others in a group and then organize context-appropriate social output.³⁴ Socially relevant information related to sociality may originate in cortical regions; recent studies examining group social communication between familiar bats revealed unique neural representations for specific individuals within the frontal cortex,³⁵ and other studies have demonstrated a role for the frontal cortex, specifically the anterior cingulate cortex (ACC), in complex, prosocial behaviors that likely facilitate group living, such as consolation.³⁶ Further, the evolution of highly prosocial phenotypes in group-living species may also be associated with circuits that inhibit the aggression many animals typically show toward conspecifics in several, if not most contexts. Specifically, the primarily GABAergic^{34,37} LS may inhibit activity in downstream, aggression-promoting regions of the brain, such as the lateral and ventromedial hypothalamus.^{38,39} LS circuitry could thereby allow species like spiny mice to engage in prosocial interactions with large groups of conspecifics regardless of context.

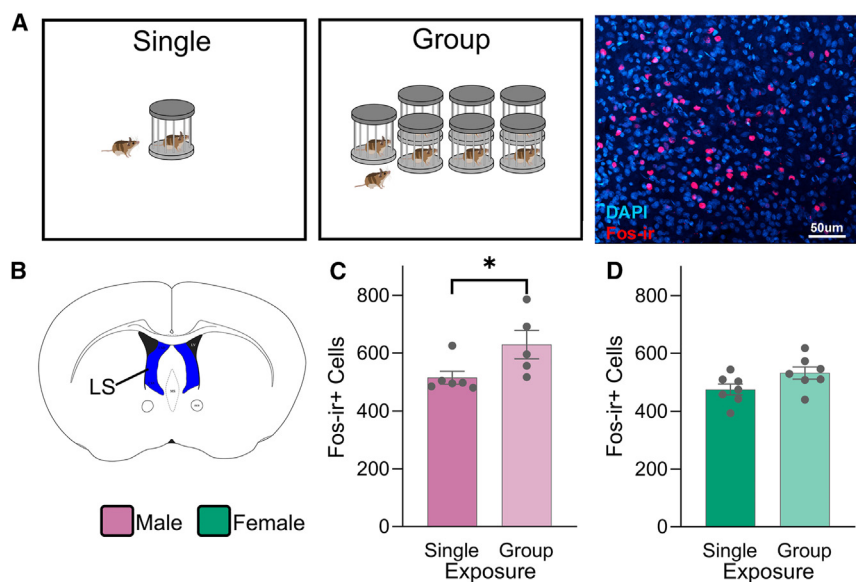


Figure 1. Lateral septum Fos responses to group size

(A) Left: illustration of single exposure condition for group size preference in the IEG study. Middle: illustration of group exposure condition for group size exposure IEG study. Right: representative histological image depicting DAPI nuclear stain (blue) and Fos-ir (red) staining within the LS. (B) Schematic depicting LS region used for analysis.

(C) In male spiny mice, the LS had significantly more Fos-ir+ cells when subjects were exposed to a large group compared with a single novel same-sex conspecific. Independent t test, $p = 0.050$ after multiple comparison corrections.

(D) In female spiny mice, the LS trended toward exhibiting more Fos-ir+ cells when subjects were exposed to a large group compared with a single novel same-sex conspecific. Independent t test, $p = 0.066$ after multiple comparison corrections. Data represented as mean \pm SEM. * $p \leq 0.05$. See also Figure S2.

Here, we contribute novel insights to the field of social neuroscience by moving beyond the delineation of circuits that mediate traditional dyadic interactions and affiliative preferences between two individuals. Specifically, we identify neural circuitry that modulates the drive to affiliate with large groups of novel peers in a non-reproductive context in male and female spiny mice. Using a combination of neural tracing techniques and immediate-early gene (IEG) studies, we first identify a circuit that potentially mediates peer grouping preferences—neuronal projections from the ACC to the LS. Next, we use chemogenetics to demonstrate that this circuit directly modulates spiny mice affiliative and investigative preferences toward larger peer groups compared with smaller ones. Further, additional tracing and IEG studies reveal that the LS may suppress aggressive behavior with novel same-sex conspecifics via action in the lateral hypothalamus (LHa), thereby enabling cohesive peer groups. Together, our data demonstrate for the first time in a mammal that, like humans, evolved to live in groups that the ACC-LS circuit is an integral mediator of peer group affiliation responses that are likely critical for the formation and possibly cohesion of complex mammalian societies.

RESULTS

The LS differentially responds to group size

To confirm that the LS is responsive to social stimuli, as has been shown in other species,^{27,40,41} we first conducted an IEG study in which four male and four female spiny mice were exposed to either a novel same-sex conspecific or a novel rubber duck. Spiny mice exposed to a novel same-sex conspecific exhibited significantly more Fos-ir+ cells in the LS compared with those exposed to a novel rubber duck ($F_{(1, 4)} = 50.223$, $p = 0.002$; Figure S1), confirming that the LS is responsive to social stimuli in spiny mice.

We next aimed to identify whether the LS differentially responds to exposure to small vs. large groups. Additionally, we examined three other brain regions that have been previously implicated in a variety of social behaviors—the medial septum

(MS; involved in social memory formation⁴²), the medial preoptic area (mPOA; crucial for parental care^{43,44}), and the BNST (facilitates grouping in birds and social vigilance in California mice^{45–47}). We first performed an IEG study in which six male spiny mice were exposed to a single novel same-sex conspecific and another six to a group of seven novel same-sex conspecifics for 30 min, followed by an additional 30 min of isolation. An identical follow-up study was later conducted in females (note that both sexes are analyzed separately due to males and females being tested on different dates). Using immunohistochemistry (IHC), we quantified the number of Fos-ir+ cells for each subject in the MS, mPOA, BNST, and LS.

In male spiny mice, there were no differences in the number of Fos-ir+ cells between the single exposure and group exposure conditions for the MS ($t_{(9)} = -1.410$, $p = 0.202$), mPOA ($t_{(9)} = -0.828$, $p = 0.429$), and BNST ($t_{(9)} = -0.270$, $p = 0.793$) (Figures S2A–S2C). However, for the LS, there was a significant difference between exposure conditions such that male spiny mice exposed to the group exhibited significantly more Fos-ir+ cells than males exposed to a single conspecific ($t_{(9)} = -2.267$, $p = 0.05$; Figure 1C). In female spiny mice, we observed no Fos expression differences between the single and group exposure conditions for the MS ($t_{(12)} = -1.515$, $p = 0.160$) and BNST ($t_{(12)} = 1.338$, $p = 0.206$) (Figures S2D and S2F). We observed a trend for the LS ($t_{(12)} = 2.025$, $p = 0.066$) (Figure 1D), suggesting that the LS may differentially process group size in females, albeit not as strongly as in males. Last, we found a significant difference for the mPOA in females, such that females exposed to the large group exhibited more Fos-ir+ cells than females exposed to a single conspecific ($t_{(12)} = 2.974$, $p = 0.012$; Figure S2E). These initial IEG studies identified the LS as a region that might play a role in regulating peer group preference in spiny mice.

LS-projecting neurons within the ACC differentially respond to peer group size

We next sought to identify regions upstream of the LS that may be differentially modulated by exposure to large groups

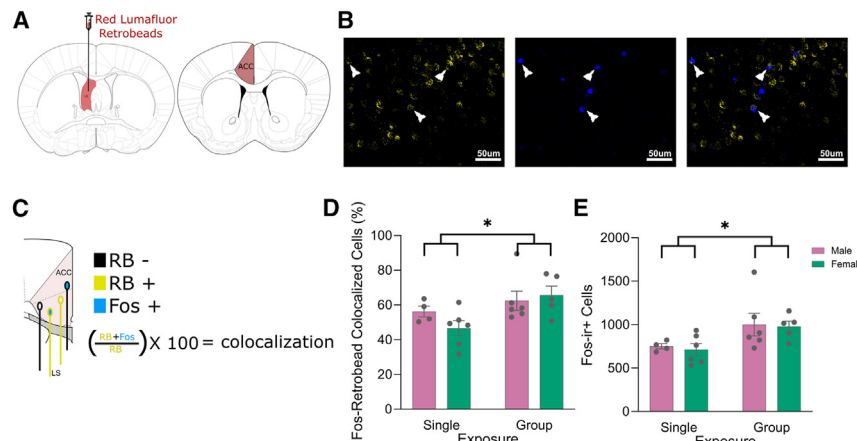


Figure 2. Lateral septum-projecting neurons within the anterior cingulate cortex differentially respond to group size

(A) Left: schematic of red retrobead injection location within the LS. Right: example schematic of area considered ACC for cell counting. (B) Representative histological images depicting retrobead (left; pseudocolored yellow), Fos-ir (middle; blue), and retrobead-Fos colocalization (right) staining within the ACC. White arrows indicate retrobead-Fos colocalized cells. (C) Left: schematic depicting possible combinations of retrobead positive or negative and Fos positive or negative neurons. Right: formula depicting how values in (D) were calculated. (D) The rostral ACC showed a greater percentage of retrobead-labeled neurons colocalized with Fos-ir in subjects exposed to a large group compared with a single novel same-sex conspecific for both

sexes. General linear model (GLM) with exposure type and sex as fixed factors. Sex, $p = 0.416$; exposure type, $p = 0.020$; interaction, $p = 0.210$. (E) The average of all ACC tissue sections quantified showed significantly higher Fos-ir expression in subjects exposed to a large group compared with a single, same-sex conspecific for both sexes. GLM with exposure type and sex as fixed factors. Sex, $p = 0.566$; exposure type, $p = 0.028$; interaction, $p = 0.305$. Data represented as mean \pm SEM. * $p \leq 0.05$. See also [Figure S3](#) and [Tables S1](#), [S2](#), and [S4](#).

compared with a single novel conspecific. To identify such regions, we repeated the IEG study design above with the addition of retrograde tracing in 12 male and 12 female spiny mice. 7 days prior to the IEG study, we performed an intracranial injection of red Lumafluor retrobeads into the LS of one hemisphere ([Figure 2A](#)). The use of retrobeads allowed for colocalizing Fos-ir expression in cell bodies of neurons projecting to the LS. This co-labeling enabled us to calculate a percentage of LS-projecting neurons that were Fos-ir+ in a given region ([Figure 2C](#)). With exposure type (single conspecific or peer group) and sex as fixed factors, we analyzed the percentage of retrobead-labeled neurons that were Fos-ir+ as well as the average number of Fos-ir+ neurons in several regions associated with social behavior in other rodents. Brains were examined for retrobead labeling from the olfactory bulb through the ventral tegmental area (VTA). Brain regions that expressed robust retrobead labeling and are well known to modulate aspects of social behavior were selected for analyses ([STAR Methods](#)). Due to differences in the number of retrobead-labeled neurons across all sections of a brain region, analyses were conducted on both rostral and caudal portions of each brain region separately. Additionally, we analyzed the percentage of retrobead-labeled neurons that were Fos-ir+ across all tissue sections of a region. For Fos-ir expression, only an average across the region was quantified.

For the anterior olfactory nucleus and piriform cortex ([Figures S3B](#) and [S3C](#)), analyses yielded no differences or any interactions for the percentage of retrobead-labeled neurons that were Fos-ir+ as well as the average number of Fos-ir+ neurons (all $p > 0.057$; [Tables S1](#) and [S2](#)). However, analysis of the rostral ACC yielded a significant difference across exposure type for the percentage of retrobead-labeled neurons that were Fos-ir+ ($F_{(1, 21)} = 6.529$, $p = 0.02$). Similarly, the average of Fos-ir expression across all ACC sections significantly differed ($F_{(1, 21)} = 5.791$, $p = 0.028$), such that both the percentage of retrobead-labeled neurons that were Fos-ir+ and the average Fos-ir expression across all ACC sections were higher for the group exposure

condition compared with the single exposure condition ([Figure 2D](#)). We observed no effects or interactions with sex for retrobead-Fos colocalization or Fos-ir expression in the ACC (all $p > 0.527$). Although there were no effects of exposure type or sex observed for analyses of the basolateral amygdala (BLA) or VTA, we found a significant interaction between exposure type and sex for BLA retrobead-Fos colocalization averaged across all sections quantified ($F_{(1, 21)} = 4.610$, $p = 0.045$; [Figure S3A](#)) and for rostral VTA retrobead-Fos colocalization ($F_{(1, 19)} = 5.113$, $p = 0.036$; [Figure S3D](#); [Table S1](#)); however, post hoc analyses with corrections did not yield any significant differences (all $p > 0.097$). The average number of retrobead+ neurons for each region can be found in [Table S4](#). These results suggest that peer group size is processed in ACC neurons that project to the LS.

Inhibition of the ACC-LS reverses affiliative large-peer-group preference in male, but not female, spiny mice

The IEG study paired with retrograde tracing identified a circuit—the ACC-LS—that responded to variation in group size. Thus, we hypothesized that the ACC-LS circuit facilitates the preference to affiliate with large groups in spiny mice. To test this hypothesis, we utilized cre-dependent inhibitory chemogenetics to determine the direct contribution of this circuit to peer group size preference. We first conducted a validation study and confirmed for the first time the efficacy of cre-dependent inhibitory designer receptors exclusively activated by designer drugs (DREADDs) in spiny mice ([STAR Methods](#); [Figure S4](#)).

In previous studies examining group size preference in spiny mice, we used a single-chambered apparatus that allowed subjects to view both the large and small groups simultaneously.^{15,22} To force more of a choice on subjects, we created a new, modified testing chamber, which required subjects to enter two distinct subchambers to access the stimulus groups. Subjects had physical access to stimulus animals via 0.312-cm-diameter holes in the subchamber walls. We utilized the validated cre-dependent inhibitory DREADDs to inhibit the ACC-LS circuitry

during this modified peer group size preference test to obtain causal evidence of the circuit's contribution to behavior when an animal has a choice to investigate and affiliate with a large or small group of novel peers. Thirty-two male and 32 female spiny mice were randomly assigned to one of four conditions: (1) Dio-hM4Di + saline, (2) Dio-hM4Di + clozapine N-oxide (CNO), (3) mCherry + saline, or (4) mCherry + CNO. Subjects underwent bilateral intracranial injections in which cre AAVs were injected into the LS for all subjects, and half of the subjects received an injection of cre-dependent Dio-hM4Di AAVs into the ACC, whereas the other half received an injection of an mCherry AAV into the ACC (Figure 3A). Five weeks after the intracranial injections, all subjects underwent two behavioral tests with an hour in between each test—a social peer group size preference test and a nonsocial group size preference test; the order of tests was counter-balanced across all four groups. For the peer group size preference test, one subchamber had two novel same-sex conspecifics and the other had eight novel same-sex conspecifics (Figure 3B). All stimulus animals were unrelated to the subject. During the nonsocial group size preference test, however, the conspecifics were replaced with novel, spiny-mouse-sized rubber ducks (Figure 4B). 30 min prior to the first test, half of the Dio-hM4Di and mCherry subjects received an intraperitoneal (i.p.) injection of saline, whereas the other half received CNO. For behavioral scoring, we quantified the amount of time each subject spent near each group (henceforth referred to as affiliation) and investigating each group. We divided the chamber into four quadrants (Figures 3B and S6A), with the quadrants closest to each group considered as “near” the group (i.e., affiliation), whereas investigation was considered as pressing one's nose up to a chamber containing a stimulus animal.

We previously showed that both male and female spiny mice preferentially investigate and affiliate with a large peer group over a small peer group in a group size preference test, reflecting their behavioral ecology to live in large groups in the wild.^{15,22} To validate that this preference was retained in our new dual-chambered apparatus, we compared the time all control subjects (i.e., all subjects excluding the Dio-hM4Di + CNO condition) affiliated with and investigated the large group compared with the small group of novel same-sex conspecifics. There was a significant effect of group for affiliation ($F_{(1,92)} = 26.755$, $p < 0.001$) and investigation ($F_{(1,92)} = 93.457$, $p < 0.001$) such that, for both sexes, spiny mice spent more time affiliating with (MD = 59.893, $p < 0.001$) and investigating (MD = 66.468, $p < 0.001$) the large group of peers compared with the small group (Figures S6B and S6D). For investigation, there was also a significant effect of sex ($F_{(1,92)} = 4.823$, $p = 0.031$) such that females investigated groups less than males (MD = 15.100, $p = 0.031$; Figure S6D). These results provide further support for the observation that spiny mice prefer affiliating with larger peer groups and show that our new testing chamber does not significantly impact group preference. Furthermore, to determine whether our group size preference test distinguishes grouping preferences of spiny mice from lab mice, we conducted a group size preference test using 12 female C57BL/6J mice—a strain of mouse that can be group housed, although high levels of aggression are typically observed, particularly for males.^{48,49} We found that while female lab mice exhibited a significant preference to investigate the large group over the small group ($t_{(11)} = 6.167$,

$p < 0.001$; Figure S7B), female lab mice exhibited no affiliation preference ($t_{(11)} = 0.445$, $p = 0.665$; Figure S7A). This captures the social-neophilic nature of many species and strains of mice^{15,50,51} yet highlights the highly affiliative nature of spiny mice. Similar to previous findings comparing spiny mice with the small-family-group-living Mongolian gerbil,²² after an initial bout of active investigation of social stimuli for both C57BL/6J mice and spiny mice, only spiny mice exhibited an affiliative preference to rest amid a large group.

To determine whether neural circuits influence behavior, specifically in a social context, we also examined spiny mouse group size preferences for rubber ducks (i.e., a nonsocial context). For all control subjects (i.e., all subjects excluding the Dio-hM4Di + CNO condition), males and females did not significantly affiliate with one group of ducks more than the other ($F_{(1,92)} = 0.088$, $p = 0.768$) but did investigate the large group of ducks more than the small group of ducks ($F_{(1,92)} = 56.159$, MD = 30.349, $p < 0.001$; Figures S6C and S6E). This suggests that spiny mice have a preference to investigate more of an object, social or nonsocial.

To test the hypothesis that the ACC-LS circuit facilitates the preference to affiliate with large groups in spiny mice, we compared behavior across Dio-hM4Di + CNO animals, mCherry + CNO animals, and AAV + saline animals. The AAV + saline group combines mCherry + saline and Dio-hM4Di + saline animals because there were no behavioral differences between animals in these conditions (all $p > 0.062$). Using the group size preference tests just described, we obtained three normalized behavior scores: (1) an affiliation score, which was based on all time spent in close proximity to the large group compared with the small group; (2) an investigation score, which was based on the time spent investigating the large group compared with the small group; and (3) an antisocial score, which was the percentage of the test the subject spent in one of the two quadrants not near a group. Positive affiliation and investigation scores reflect more affiliation/investigation with the large group, whereas negative scores reflect more affiliation/investigation with the small group.

In the peer group size preference test, we found a main effect of condition (i.e., AAV + saline vs. mCherry + CNO vs. Dio-hM4Di + CNO) ($F_{(2,54)} = 19.369$, $p < 0.001$, $\eta_p^2 = 0.421$) and a main effect of sex for the affiliation score ($F_{(1,54)} = 7.209$, $p = 0.010$, $\eta_p^2 = 0.118$). There was also a significant interaction between condition and sex for the affiliation score ($F_{(2,54)} = 5.720$, $p = 0.006$, $\eta_p^2 = 0.175$; Figure 3C). Post hoc analyses revealed that only male Dio-hM4Di + CNO subjects reversed their affiliation scores, and thus preferred affiliating with the small peer group, compared with the mCherry + CNO (MD = -0.632 , $p < 0.001$) and AAV + saline (MD = -0.683 , $p < 0.001$) conditions, whereas females across conditions exhibited no significant difference in their affiliation scores (all $p > 0.116$). We also observed a main effect of condition for the investigation score ($F_{(2,54)} = 12.853$, $p < 0.001$, $\eta_p^2 = 0.323$; Figure 3D). Post hoc analyses showed that Dio-hM4Di + CNO subjects of both sexes exhibited a decreased preference for investigating the large group of peers compared with mCherry + CNO (MD = -0.340 , $p < 0.001$) and AAV + saline (MD = -0.340 , $p < 0.001$) conditions. However, the antisocial score was not significantly different across experimental conditions ($F_{(2,54)} = 0.181$, $p = 0.806$, $\eta_p^2 = 0.008$;

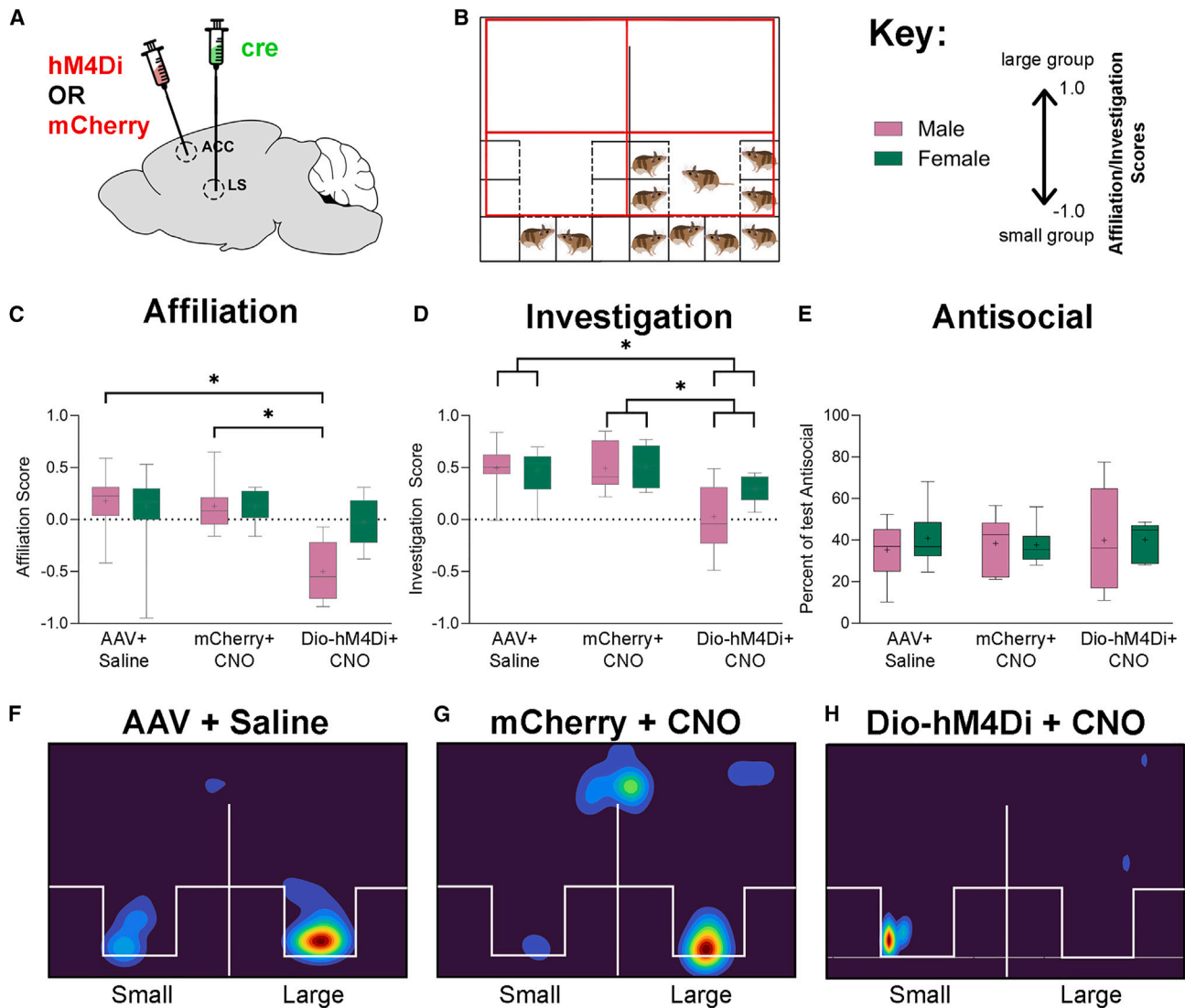


Figure 3. The anterior cingulate cortex to lateral septum circuit modulates social peer group size preference in a sex-specific manner

(A) Schematic of cre (LS) and hM4Di (ACC) AAV injection locations.

(B) Schematic depicting a top-down view of the group size preference testing during a social peer group size preference test. Red boxes indicate quadrants for scoring.

(C) For Dio-hM4Di + CNO subjects, inhibition of ACC-LS circuitry reversed the affiliative preference for larger social peer groups in male, but not female, spiny mice. GLM with condition (AAV + saline, mCherry + CNO, and Dio-hM4Di + CNO) and sex (male or female) as fixed factors. Sex, $p = 0.010$; condition, $p < 0.001$; interaction, $p = 0.006$. Female-condition interaction, all $p > 0.116$; male-condition interaction, all $p < 0.001$.

(D) For Dio-hM4Di + CNO subjects, inhibition of ACC-LS circuitry resulted in less investigation of the large group for male and female spiny mice. GLM with condition (AAV + saline, mCherry + CNO, and Dio-hM4Di + CNO) and sex (male or female) as fixed factors. Sex, $p = 0.113$; condition, $p < 0.001$; interaction, $p = 0.190$.

(E) Inhibition of ACC-LS circuitry did not affect the percentage of test time spent away from either group (i.e., antisocial behavior). GLM with condition (AAV + saline, mCherry + CNO, and Dio-hM4Di + CNO) and sex (male or female) as fixed factors, $p > 0.747$.

(F–H) Representative heatmaps of male subject location during the social peer group size preference test for the AAV + saline, mCherry + CNO, and Dio-hM4Di + CNO conditions.

Data represented as boxplots with a median line and a mean indicated by + in the center of each bar. $*p \leq 0.05$.

See also Figures S5–S8.

Figure 3E). Last, because CNO can have off-target effects and influence locomotion,^{52,53} to specifically examine whether CNO influenced movement, we collapsed groups and sexes to examine animals injected with saline compared with those

injected with CNO. This yielded no effect of injection type on velocity or distance traveled (all $p > 0.270$; Figure S8), showing that CNO did not significantly influence movement in our test. Together, these findings indicate that activation of the ACC-LS

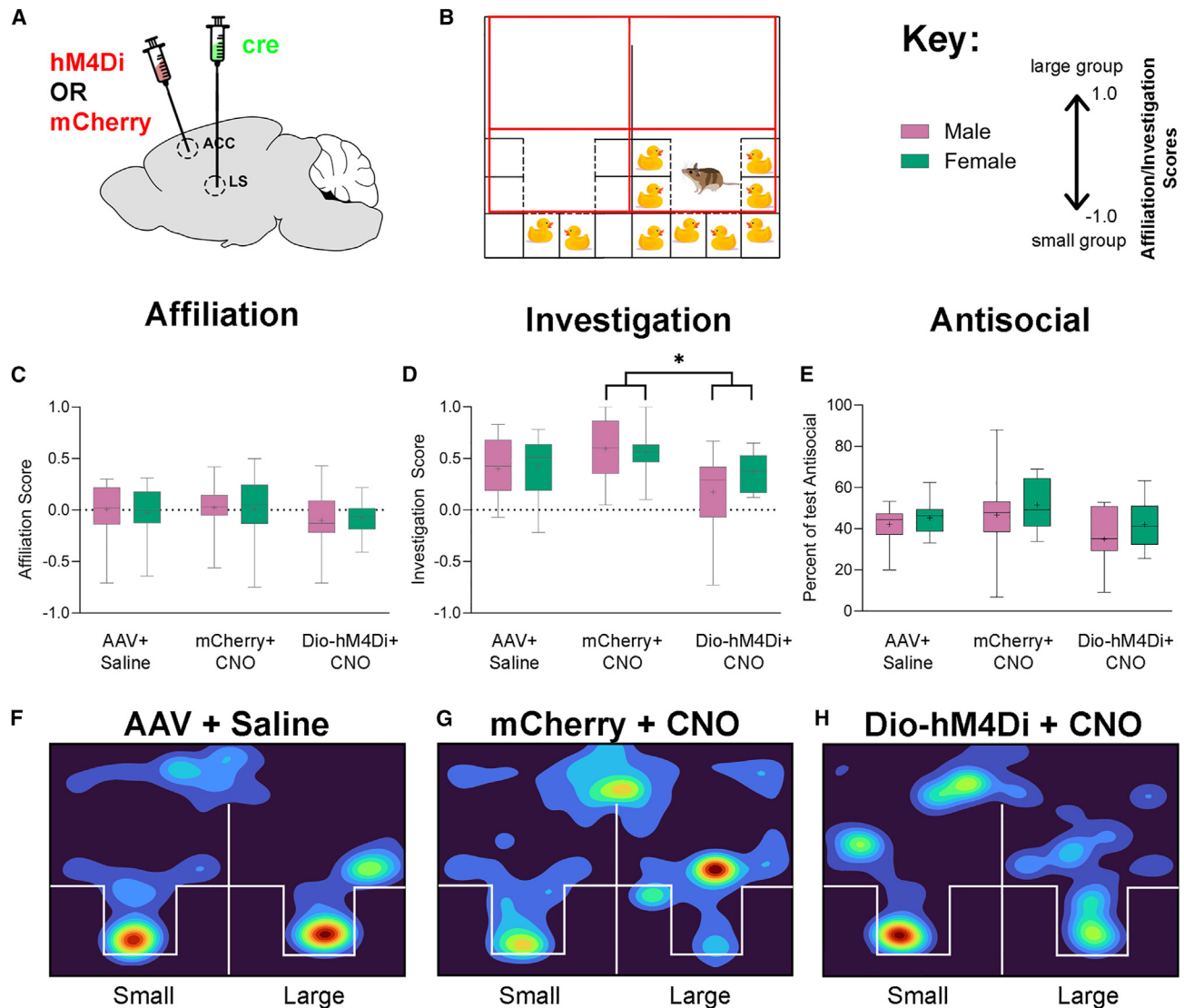


Figure 4. Anterior cingulate cortex to lateral septum circuit effects on behavior during nonsocial group size preference tests

(A) Schematic of *cre* (LS) and Dio-hM4Di (ACC) AAV injection locations.
 (B) Schematic depicting a top-down view of the group size preference testing during a nonsocial group size preference test, with rubber ducks acting as a nonsocial stimulus. Red boxes indicate quadrants for scoring.
 (C) Inhibition of ACC-LS circuitry did not affect affiliative preferences during a nonsocial group size preference test. Condition (AAV + saline, mCherry + CNO, and Dio-hM4Di + CNO) and sex (male or female) as fixed factors, all $p > 0.562$.
 (D) For Dio-hM4Di + CNO subjects, inhibition of ACC-LS circuitry decreased the preference to investigate the large group of novel rubber ducks compared with mCherry + CNO control animals but not to AAV + saline control animals. Condition (AAV + saline, mCherry + CNO, and Dio-hM4Di + CNO) and sex (male or female) as fixed factors. Condition, $p = 0.027$; sex, $p = 0.453$; interaction, $p = 0.587$.
 (E) Inhibition of ACC-LS circuitry did not affect time spent away from novel objects (i.e., antisocial behavior) during a nonsocial group size preference test. Condition (AAV + saline, mCherry + CNO, and Dio-hM4Di + CNO) and sex (male or female) as fixed factors, all $p > 0.084$.
 (F–H) Representative heatmaps of male subject location during the nonsocial peer group size preference test for the AAV + saline, mCherry + CNO, and Dio-hM4Di + CNO conditions.
 Data represented as boxplots with a median line and a mean indicated by + in the center of each bar. $*p \leq 0.05$.
 See also [Figures S4](#) and [S5](#).

circuit in male spiny mice is necessary for their ethologically relevant preference to affiliate with a large peer group. Furthermore, inactivation of this circuit did not induce a preference to be antisocial but instead affected social preferences in a sex-specific manner.

Inhibition of the ACC-LS does not uniformly alter behavior during a nonsocial group size preference test

To determine whether the effects of inhibiting the ACC-LS were specific to a social context or rather affect general responses to large quantities of objects, all male and female spiny mice also

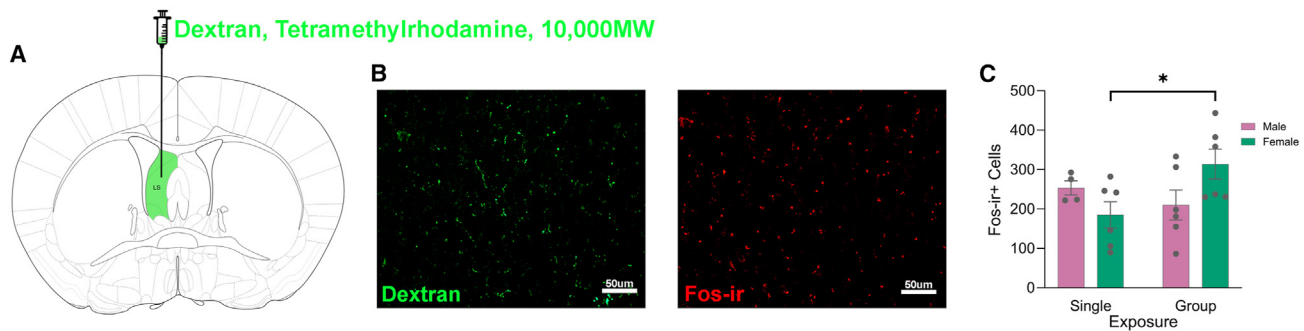


Figure 5. The lateral hypothalamus receives projections from the lateral septum and differentially responds to group size in a sex-specific manner

(A) Schematic of high-molecular-weight dextran injection location within the LS.

(B) Representative histological images depicting dextran (right) and Fos-ir (left) staining within the LHa.

(C) The LHa had significantly higher Fos-ir in subjects exposed to a large group compared with a single, same-sex conspecific for females, but not males. GLM with exposure type and sex as fixed factors. Sex, $p = 0.339$; exposure type, $p = 0.252$; interaction, $p = 0.028$. Female exposure, $p = 0.015$; male exposure, $p = 0.428$.

Data represented as mean \pm SEM. * $p \leq 0.05$.

See also [Figure S9](#) and [Table S3](#).

underwent a nonsocial group size preference test, for which, instead of novel same-sex conspecifics as stimuli, the two stimulus groups were comprised of novel, spiny-mouse-sized rubber ducks ([Figure 4B](#)). We found no effects of or interactions between condition and sex for the affiliation score (all $p > 0.562$; [Figure 4C](#)). However, we observed a main effect of condition for the investigation score ($F_{(2, 55)} = 3.850$, $p = 0.027$, $\eta_p^2 = 0.123$; [Figure 4D](#)). Post hoc analyses showed that Dio-hM4Di + CNO subjects of both sexes exhibited a decreased preference for investigating the large group of rubber ducks compared with the mCherry + CNO condition ($MD = -0.304$, $p = 0.024$) but not compared with the AAV + saline ($MD = -0.146$, $p = 0.394$) condition. Further, we observed no effects of or interactions of condition and sex for time spent away from the stimulus rubber duck groups (i.e., “antisocial” behavior; all $p > 0.084$; [Figure 4E](#)). These results for the nonsocial group size preference test indicate the ACC-LS’s modulation of affiliative-peer-group preferences is restricted to a social context. However, the ACC-LS circuit may also play a role in nonsocial investigation; this remains unclear, given that the experimental inhibition condition did not significantly differ from all control groups.

The LHa—a downstream target of the LS—responds to peer group size in a sex-specific manner

Finally, because social group size preference and related behaviors likely require complex interactions between neural circuits spanning more than two regions, we sought to identify brain regions downstream of the LS that respond to variation in peer group size. In the retrograde group size IEG study described earlier, in addition to an injection of red retrobeads, subjects also received a unilateral injection of green, high-molecular-weight dextran, an anterograde tracing molecule that labels downstream synaptic terminals, into the LS ([Figures 5A and 5B](#)). We quantified the average number of Fos-ir+ cells in regions that contained robust dextran labeling that have been previously implicated in rodent social behavior ([STAR Methods](#)).

The majority of regions analyzed, including the preoptic area and nucleus accumbens, among others, showed no differences between single conspecific and peer group exposure conditions (all $p > 0.069$; [Figure S9](#); [Table S3](#)). However, we identified a significant interaction for Fos-ir in the LHa ($F_{(1, 18)} = 5.725$, $p = 0.028$), with females ($MD = 128.556$, $p = 0.015$) but not males ($MD = 43.50$, $p = 0.428$) exhibiting a significantly larger number of Fos-ir+ cells in the peer group exposure compared with the single conspecific exposure ([Figure 5C](#)). Together, our results suggest that, while ACC-LS circuitry modulates investigation of larger peer groups in both sexes, the same circuit only promotes the preference to affiliate with larger peer groups in males. Further, activity within the ACC-LS circuitry may alter the downstream activity of the LHa in a sex-specific manner, potentially differentially influencing affiliative behavior and/or preferences in males and females.

DISCUSSION

Here, we show for the first time in a group-living mammal that the ACC-LS regulates grouping preferences. Through IEG and tracing studies, we showed that neurons in the ACC responded more to larger than smaller groups of novel same-sex conspecifics. This higher response in the ACC was also observed specifically in neurons projecting to the LS. Through chemogenetic inhibition of the ACC-LS circuit, we observed a significant decrease in the preference for male and female spiny mice to investigate large peer groups and a sex-specific reversal of affiliative preferences during a social peer group size preference test. Further, ACC-LS modulation of affiliative group size preference was specific to a social context, as inhibition of this circuit did not influence affiliative behavior in a nonsocial group size preference test. The ACC-LS may influence investigative behavior in nonsocial contexts; however, here we found that animals that had an inhibited ACC-LS circuit did not significantly differ in nonsocial investigative behavior compared with all control

groups; therefore, we cannot definitively conclude whether the ACC-LS modulates nonsocial investigation.

To our knowledge, this is the first example of a specific neural circuit modulating group size preferences, particularly in a non-reproductive context. For species that live in large groups, including humans, the majority of social interactions individuals engage in on a daily basis are likely to be non-reproductive. To further our understanding of peer group interactions, including their dysregulation, it is crucial to have a solid understanding of the circuits driving the base motivation to non-reproductively associate with others. Although no other researchers have specifically manipulated the ACC-LS circuit in social group size contexts, several studies have examined functions of these brain regions separately from each other. Indeed, both the LS and ACC have been implicated in numerous social behaviors across species. The LS is involved in grouping in birds,^{13,54} kin/social recognition in rodents,^{21,30–32} and aggression in rats and mice.^{28,29} The ACC promotes consolation³⁶ and helping^{55–57} behavior, modulates anxiety and aggression,⁵⁸ and regulates different forms of attention,^{59,60} which may affect how subjects attend to, assess the numbers of, and interact with conspecifics. For an organism to display a social preference, they must (1) attend to social stimuli consisting of at least two choices, (2) process these stimuli and discriminate between them, and (3) affiliate with the most contextually relevant stimulus. Because affiliating with a large group is ecologically relevant for spiny mice, the ACC may function to direct attention toward large groups as they likely afford more benefits compared with smaller groups. Additionally, given that the LS is involved in social recognition in rats³⁰ and promotes affiliation in voles and finches,^{13,32} the LS in spiny mice may facilitate social discrimination of small vs. large peer groups and/or promote, via specific neural activity, affiliation with the most beneficial group. Together, the ACC-LS circuit may modulate group size preference by regulating attention to, discrimination between, and behavioral outputs toward large groups in spiny mice. Because chemogenetic inhibition of the ACC-LS circuit did not clearly influence behavior in the nonsocial group size preference test, this circuit is likely not involved in the subjects' ability to process numerosity^{61,62} or global attention to any type of stimuli. Indeed, this circuit appears to be specific to social stimuli and may potentially be involved in social attentional processes.

We have previously shown that both male and female spiny mice exhibit a robust preference to affiliate with and investigate larger over smaller groups.^{15,22} Here, the preference to investigate larger peer groups was decreased via inhibition of the ACC-LS in both sexes, but only in males did inhibiting this circuit reverse their affiliative preference away from larger and toward smaller peer groups. Although ACC neurons that project to the LS were significantly more responsive to a large than small group in both males and females, the IEG study examining LS neural responses (i.e., not those specific to ACC projections) yielded only a trend for female spiny mice exposed to either a large or a small group of same-sex conspecifics. Thus, it possible that while group size information sent to the LS from the ACC may be similar in males and females, how the LS responds to and/or processes group size information is distinct between male and female spiny mice. This is consistent with studies in other species that have reported sex differences in LS social function.^{28,63–66} Notably, the group size preference tests here were conducted

with novel same-sex conspecifics. In a former study, we showed that during social preference tests both males and females prefer to affiliate with novel males over novel females.¹⁵ In the current study, spiny mice could only affiliate with same-sex conspecifics, so the drive to be affiliative with same-sex peers may have been greater in males than in females because females did not have the option to affiliate with their preferred sex while males did. Thus, the ACC-LS circuit may have evolved to promote social investigation in both sexes and was subsequently co-opted in male spiny mice to also drive affiliation preferences. Although field studies of grouping are lacking in spiny mice, several species, such as the African striped mouse,⁶⁷ form bachelor groups during different phases of their life history, and, thus, in some species the drive to affiliate with same-sex peers may be greater in males than in females.

Downstream of the LS, the LH_a exhibited greater Fos-ir expression in response to a large group compared with a small group of same-sex peers in female, but not male, spiny mice. The LH_a has been implicated in aggression in several rodent species^{68,69} as well as social dominance in C57BL/6J mice.⁷⁰ Notably, female spiny mice are dominant over males and same-sex aggression is more common in female-female co-housed cages than in male-male cages.⁷¹ Thus, while male spiny mice may find a large group of same-sex conspecifics simply rewarding, females may have a more complex response to the same context, resulting in increased focus on social hierarchy or potential threats. Alternatively, the sex effect of chemogenetic inhibition of the ACC-LS on affiliative preferences here could be due to differences in incentive values in male and female spiny mice, although we observed no significant differences in Fos expression based on exposure condition given that the LS is connected to reward circuitry.

The drive to affiliate with a large peer group is likely a critical precursor to other, more complex, grouping behaviors. Indeed, without an initial preference to form groups, advantageous behaviors such as group foraging, co-parenting, organized defense, or homeostatic regulation may not frequently occur in natural environments. This initial preference may be innate but could equally be learned early in life. Although large groups in the wild are often comprised of mixed-sex individuals, disentangling the motivation to mate from general peer affiliation can help elucidate distinct mechanisms that contribute toward effective grouping and enable cooperative behaviors between same-sex peers. By revealing neural underpinnings of the preference to investigate and affiliate with large groups, we have identified brain regions of interest that may influence other more complex grouping behaviors. Further, by using an ethologically relevant organism for the study of grouping behavior, we uncovered a neural circuit dedicated to social preference that functions in a sex-specific manner. Our results highlight the ACC-LS as a promising circuit for the regulation of complex social behaviors in large group-living species.

RESOURCE AVAILABILITY

Lead contact

Further information and requests for resources and reagents should be directed to, and will be fulfilled by, the lead contact, A.M. Kelly (aubrey.kelly@emory.edu).

Materials availability

This study did not generate unique reagents.

Data and code availability

- IHC cell counts and behavioral data have been deposited at Dryad and are publicly available as of the date of publication. Accession numbers are listed in the [key resources table](#).
- This paper does not report original code.
- Any additional information required to reanalyze the data reported in this paper is available from the [lead contact](#) upon request.

ACKNOWLEDGMENTS

We would like to thank Nicklas Gose for assistance with Ethovision behavioral video scoring. We would like to acknowledge funding from the Klingenstein-Simons Foundation (Fellowship Award in Neuroscience to A.M.K.), the National Institute of Arthritis and Musculoskeletal and Skin Diseases (R01AR070313 to A.W.S.), and the National Science Foundation (IOS-1353713 to A.W.S. and IOS-2310626 to A.M.K.). B.A.F. was supported by the Department of Defense (DoD) through the National Defense Science & Engineering Graduate (NDSEG) fellowship program.

AUTHOR CONTRIBUTIONS

B.A.F. designed the study, conducted behavioral tests, scored behavioral videos, conducted stereotaxic surgeries, cryosectioned brains, conducted immunohistochemistry, conducted microscopy and cell counts, analyzed the data, and wrote the manuscript. M.M. and A.W.S. provided feedback on and edited the manuscript. A.M.K. designed the study, wrote the manuscript, and as principal investigator, obtained the funding.

DECLARATION OF INTERESTS

The authors declare no competing interests.

STAR★METHODS

Detailed methods are provided in the online version of this paper and include the following:

- [KEY RESOURCES TABLE](#)
- [EXPERIMENTAL MODEL AND STUDY PARTICIPANT DETAILS](#)
 - Spiny mouse, *Acomys dimidiatus* (formerly known as *Acomys cahirinus*)
- [METHOD DETAILS](#)
 - Stereotaxic injections
 - Validation of cre-dependent inhibitory DREADDs in spiny mice
 - Behavioral Assays
- [QUANTIFICATION AND STATISTICAL ANALYSIS](#)

SUPPLEMENTAL INFORMATION

Supplemental information can be found online at <https://doi.org/10.1016/j.cub.2024.08.019>.

Received: March 19, 2024

Revised: July 17, 2024

Accepted: August 13, 2024

Published: September 11, 2024

REFERENCES

1. Berdahl, A.M., Kao, A.B., Flack, A., Westley, P.A.H., Codling, E.A., Couzin, I.D., Dell, A.I., and Biro, D. (2018). Collective animal navigation and migratory culture: from theoretical models to empirical evidence. *Philos. Trans. R. Soc. Lond. B Biol. Sci.* 373, 20170009. <https://doi.org/10.1098/rstb.2017.0009>.
2. Markham, A.C., Gesquiere, L.R., Alberts, S.C., and Altmann, J. (2015). Optimal group size in a highly social mammal. *Proc. Natl. Acad. Sci. USA* 112, 14882–14887. <https://doi.org/10.1073/pnas.1517794112>.
3. Bettridge, C.M., and Dunbar, R.I.M. (2012). Predation as a determinant of minimum group size in baboons. *Folia Primatol. (Basel)* 83, 332–352. <https://doi.org/10.1159/000339808>.
4. Burger, J., and Gochfeld, M. (2001). Smooth-billed ani (*Crotophaga ani*) predation on butterflies in Mato Grosso, Brazil: risk decreases with increased group size. *Behav. Ecol. Sociobiol.* 49, 482–492. <https://doi.org/10.1007/s002650100327>.
5. White, A.M. (2010). A pigheaded compromise: do competition and predation explain variation in warthog group size? *Behav. Ecol.* 21, 485–492. <https://doi.org/10.1093/beheco/arp009>.
6. Heymann, E.W., and Soini, P. (1999). Offspring number in pygmy marmosets, *Cebuella pygmaea*, in relation to group size and the number of adult males. *Behav. Ecol. Sociobiol.* 46, 400–404. <https://doi.org/10.1007/s002650050635>.
7. Peacock, M., White, A., and Cameron, E. (2010). Grouping patterns in warthogs, *Phacochoerus africanus*: is communal care of young enough to explain sociality? *Behaviour* 147, 1–18. <https://doi.org/10.1163/000579509X12459309054841>.
8. White, A.M., and Cameron, E.Z. (2011). Fitness consequences of maternal rearing strategies in warthogs: influence of group size and composition. *J. Zool.* 285, 77–84. <https://doi.org/10.1111/j.1469-7998.2011.00816.x>.
9. Cook, C.N., Kaspar, R.E., Flaxman, S.M., and Breed, M.D. (2016). Rapidly changing environment modulates the thermoregulatory fanning response in honeybee groups. *Anim. Behav.* 115, 237–243. <https://doi.org/10.1016/j.anbehav.2016.03.014>.
10. Fletcher, L.E. (2009). Examining potential benefits of group living in a sawfly larva, *Perga affinis*. *Behav. Ecol.* 20, 657–664. <https://doi.org/10.1093/beheco/arp048>.
11. Lihoreau, M., Zimmer, C., and Rivault, C. (2007). Kin recognition and incest avoidance in a group-living insect. *Behav. Ecol.* 18, 880–887. <https://doi.org/10.1093/beheco/arm046>.
12. Warburg, I., Whitford, W.G., and Steinberger, Y. (2017). Colony size and foraging strategies in desert seed harvester ants. *J. Arid Environ.* 145, 18–23. <https://doi.org/10.1016/j.jaridenv.2017.04.016>.
13. Goodson, J.L., Schrock, S.E., Klatt, J.D., Kabelik, D., and Kingsbury, M.A. (2009). Mesotocin and nonapeptide receptors promote estrildid flocking behavior. *Science* 325, 862–866. <https://doi.org/10.1126/science.1174929>.
14. Leighton, G.M. (2014). Sex and individual differences in cooperative nest construction of sociable weavers *Philetairus socius*. *J. Ornithol.* 155, 927–935. <https://doi.org/10.1007/s10336-014-1075-3>.
15. Fricker, B.A., Seifert, A.W., and Kelly, A.M. (2022). Characterization of social behavior in the spiny mouse, *Acomys cahirinus*. *Ethology* 128, 26–40. <https://doi.org/10.1111/eth.13234>.
16. Khera, M., Arbuckle, K., Hoffman, J.I., Sanderson, J.L., Cant, M.A., and Nichols, H.J. (2021). Cooperatively breeding banded mongooses do not avoid inbreeding through familiarity-based kin recognition. *Behav. Ecol. Sociobiol.* 75, 135. <https://doi.org/10.1007/s00265-021-03076-3>.
17. Quirici, V., Faugeron, S., Hayes, L.D., and Ebensperger, L.A. (2011). Absence of kin structure in a population of the group-living rodent *Octodon degus*. *Behav. Ecol.* 22, 248–254. <https://doi.org/10.1093/beheco/arp196>.
18. Shargal, E., Kronfeld-Schor, N., and Dayan, T. (2000). Population biology and spatial relationships of coexisting spiny mice (*acomys*) in Israel. *J. Mammal.* 81, 1046–1052. [https://doi.org/10.1644/1545-1542\(2000\)081<1046:PBASRO>2.0.CO;2](https://doi.org/10.1644/1545-1542(2000)081<1046:PBASRO>2.0.CO;2).
19. Shkolnik, A., and Borut, A. (1969). Temperature and water relations in two species of spiny mice (*acomys*). *J. Mammal.* 50, 245–255. <https://doi.org/10.2307/1378340>.

20. Houghton, C.L., Gawriluk, T.R., and Seifert, A.W. (2016). The biology and husbandry of the african spiny mouse (*Acomys cahirinus*) and the research uses of a laboratory colony. *J. Am. Assoc. Lab. Anim. Sci.* 55, 9–17.
21. Fricker, B.A., Ho, D., Seifert, A.W., and Kelly, A.M. (2023). Biased brain and behavioral responses towards kin in males of a communally breeding species. *Sci. Rep.* 13, 17040. <https://doi.org/10.1038/s41598-023-44257-6>.
22. Gonzalez Abreu, J.A., Rosenberg, A.E., Fricker, B.A., Wallace, K.J., Seifert, A.W., and Kelly, A.M. (2022). Species-typical group size differentially influences social reward neural circuitry during nonreproductive social interactions. *iScience* 25, 104230. <https://doi.org/10.1016/j.isci.2022.104230>.
23. Frynta, D., Cizkova, B., and Šumbera, R. (2011). A new member or an intruder: how do Sinai spiny mouse (*Acomys dimidiatus*) families respond to a male newcomer? *Behaviour* 148, 889–908. <https://doi.org/10.1163/000579511X583385>.
24. Slotnick, B.M., McMullen, M.F., and Fleischer, S. (1973). Changes in emotionality following destruction of the septal area in albino mice. *Brain Behav. Evol.* 8, 241–252. <https://doi.org/10.1159/000124357>.
25. McDonald, M.M., Markham, C.M., Norvelle, A., Albers, H.E., and Huhman, K.L. (2012). GABAA receptor activation in the lateral septum reduces the expression of conditioned defeat and increases aggression in Syrian hamsters. *Brain Res.* 1439, 27–33. <https://doi.org/10.1016/j.brainres.2011.12.042>.
26. Albert, D.J., and Chew, G.L. (1980). The septal forebrain and the inhibitory modulation of attack and defense in the rat. A review. *Behav. Neural Biol.* 30, 357–388. [https://doi.org/10.1016/s0163-1047\(80\)91247-9](https://doi.org/10.1016/s0163-1047(80)91247-9).
27. Menon, R., Süß, T., Oliveira, V.E.M., Neumann, I.D., and Bludau, A. (2022). Neurobiology of the lateral septum: regulation of social behavior. *Trends Neurosci.* 45, 27–40. <https://doi.org/10.1016/j.tins.2021.10.010>.
28. Oliveira, V.E.M., Lukas, M., Wolf, H.N., Durante, E., Lorenz, A., Mayer, A.L., Bludau, A., Bosch, O.J., Grinevich, V., Egger, V., et al. (2021). Oxytocin and vasopressin within the ventral and dorsal lateral septum modulate aggression in female rats. *Nat. Commun.* 12, 2900. <https://doi.org/10.1038/s41467-021-23064-5>.
29. Wong, L.C., Wang, L., D'Amour, J.A., Yumita, T., Chen, G., Yamaguchi, T., Chang, B.C., Bernstein, H., You, X., Feng, J.E., et al. (2016). Effective modulation of male aggression through lateral septum to medial hypothalamus projection. *Curr. Biol.* 26, 593–604. <https://doi.org/10.1016/j.cub.2015.12.065>.
30. Clemens, A.M., Wang, H., and Brecht, M. (2020). The lateral septum mediates kinship behavior in the rat. *Nat. Commun.* 11, 3161. <https://doi.org/10.1038/s41467-020-16489-x>.
31. Bychowski, M.E., Mena, J.D., and Auger, C.J. (2013). Vasopressin infusion into the lateral septum of adult male rats rescues progesterone-induced impairment in social recognition. *Neuroscience* 246, 52–58. <https://doi.org/10.1016/j.neuroscience.2013.04.047>.
32. Sailer, L.L., Park, A.H., Galvez, A., and Ophir, A.G. (2022). Lateral septum DREADD activation alters male prairie vole prosocial and antisocial behaviors, not partner preferences. *Commun. Biol.* 5, 1299. <https://doi.org/10.1038/s42003-022-04274-z>.
33. Kelly, A.M., Ong, J.Y., Witmer, R.A., and Ophir, A.G. (2020). Paternal deprivation impairs social behavior putatively via epigenetic modification to lateral septum vasopressin receptor. *Sci. Adv.* 6, eabb9116. <https://doi.org/10.1126/sciadv.abb9116>.
34. Besnard, A., and Leroy, F. (2022). Top-down regulation of motivated behaviors via lateral septum sub-circuits. *Mol. Psychiatry* 27, 3119–3128. <https://doi.org/10.1038/s41380-022-01599-3>.
35. Rose, M.C., Styr, B., Schmid, T.A., Elie, J.E., and Yartsev, M.M. (2021). Cortical representation of group social communication in bats. *Science* 374, eaba9584. <https://doi.org/10.1126/science.aba9584>.
36. Burkett, J.P., Andari, E., Johnson, Z.V., Curry, D.C., de Waal, F.B.M., and Young, L.J. (2016). Oxytocin-dependent consolation behavior in rodents. *Science* 351, 375–378. <https://doi.org/10.1126/science.aac4785>.
37. Mahadevia, D., Saha, R., Manganaro, A., Chuhma, N., Ziolkowski-Blake, A., Morgan, A.A., Dumitriu, D., Rayport, S., and Ansorge, M.S. (2021). Dopamine promotes aggression in mice via ventral tegmental area to lateral septum projections. *Nat. Commun.* 12, 6796. <https://doi.org/10.1038/s41467-021-27092-z>.
38. Wang, D., Pan, X., Zhou, Y., Wu, Z., Ren, K., Liu, H., Huang, C., Yu, Y., He, T., Zhang, X., et al. (2023). Lateral septum-lateral hypothalamus circuit dysfunction in comorbid pain and anxiety. *Mol. Psychiatry* 28, 1090–1100. <https://doi.org/10.1038/s41380-022-01922-y>.
39. Deng, K., Yang, L., Xie, J., Tang, H., Wu, G.-S., and Luo, H.-R. (2019). Whole-brain mapping of projection from mouse lateral septal nucleus. *Biol. Open* 8, bio043554. <https://doi.org/10.1242/bio.043554>.
40. Edwards, S.C., Hall, Z.J., Ihalaenen, E., Bishop, V.R., Nicklas, E.T., Healy, S.D., and Meddle, S.L. (2020). Neural circuits underlying nest building in male zebra finches. *Integr. Comp. Biol.* 60, 943–954. <https://doi.org/10.1093/icb/icaa108>.
41. Stednitz, S.J., McDermott, E.M., Ncube, D., Tallafuss, A., Eisen, J.S., and Washbourne, P. (2018). Forebrain control of behaviorally driven social orienting in zebrafish. *Curr. Biol.* 28, 2445–2451.e3. <https://doi.org/10.1016/j.cub.2018.06.016>.
42. Griguoli, M., and Pimpinella, D. (2022). Medial septum: relevance for social memory. *Front. Neural Circuits* 16, 965172. <https://doi.org/10.3389/fncir.2022.965172>.
43. Champagne, F.A., Weaver, I.C.G., Diorio, J., Sharma, S., and Meaney, M.J. (2003). Natural variations in maternal care are associated with estrogen receptor α expression and estrogen sensitivity in the medial preoptic area. *Endocrinology* 144, 4720–4724. <https://doi.org/10.1210/en.2003-0564>.
44. Rilling, J.K., and Young, L.J. (2014). The biology of mammalian parenting and its effect on offspring social development. *Science* 345, 771–776. <https://doi.org/10.1126/science.1252723>.
45. Kelly, A.M., Kingsbury, M.A., Hoffbühr, K., Schrock, S.E., Waxman, B., Kabelik, D., Thompson, R.R., and Goodson, J.L. (2011). Vasotocin neurons and septal V1a-like receptors potently modulate songbird flocking and responses to novelty. *Horm. Behav.* 60, 12–21. <https://doi.org/10.1016/j.yhbeh.2011.01.012>.
46. Luo, P.X., Manning, C.E., Fass, J.N., Williams, A.V., Hao, R., Campi, K.L., and Trainor, B.C. (2021). Sex-specific effects of social defeat stress on miRNA expression in the anterior BNST. *Behav. Brain Res.* 401, 113084. <https://doi.org/10.1016/j.bbr.2020.113084>.
47. Luo, P.X., Zakharenkov, H.C., Torres, L.Y., Rios, R.A., Gegenhuber, B., Black, A.M., Xu, C.K., Minie, V.A., Tran, A.M., Tollkuhn, J., et al. (2022). Oxytocin receptor behavioral effects and cell types in the bed nucleus of the stria terminalis. *Horm. Behav.* 143, 105203. <https://doi.org/10.1016/j.yhbeh.2022.105203>.
48. Horii, Y., Nagasawa, T., Sakakibara, H., Takahashi, A., Tanave, A., Matsumoto, Y., Nagayama, H., Yoshimi, K., Yasuda, M.T., Shimoi, K., et al. (2017). Hierarchy in the home cage affects behaviour and gene expression in group-housed C57BL/6 male mice. *Sci. Rep.* 7, 6991. <https://doi.org/10.1038/s41598-017-07233-5>.
49. Deacon, R.M.J. (2006). Housing, husbandry and handling of rodents for behavioral experiments. *Nat. Protoc.* 1, 936–946. <https://doi.org/10.1038/nprot.2006.120>.
50. Rashid, M., Thomas, S., Isaac, J., Karkare, S., Klein, H., and Murugan, M. (2024). A ventral hippocampal-lateral septum pathway regulates social novelty preference. Preprint at bioRxiv. <https://doi.org/10.1101/2024.02.28.582638>.
51. Pearson, B.L., Defensor, E.B., Blanchard, D.C., and Blanchard, R.J. (2010). C57BL/6J mice fail to exhibit preference for social novelty in the three-chamber apparatus. *Behav. Brain Res.* 213, 189–194. <https://doi.org/10.1016/j.bbr.2010.04.054>.
52. Gomez, J.L., Bonaventura, J., Lesniak, W., Mathews, W.B., Sysa-Shah, P., Rodriguez, L.A., Ellis, R.J., Richie, C.T., Harvey, B.K., Dannals, R.F., et al. (2017). Chemogenetics revealed: DREADD occupancy and

- activation via converted clozapine. *Science* 357, 503–507. <https://doi.org/10.1126/science.aan2475>.
53. Ilg, A.-K., Enkel, T., Bartsch, D., and Böhner, F. (2018). Behavioral effects of acute systemic low-dose clozapine in wild-type rats: implications for the use of DREADDs in behavioral neuroscience. *Front. Behav. Neurosci.* 12, 173. <https://doi.org/10.3389/fnbeh.2018.00173>.
54. Goodson, J.L., and Kabelik, D. (2009). Dynamic limbic networks and social diversity in vertebrates: from neural context to neuromodulatory patterning. *Front. Neuroendocrinol.* 30, 429–441. <https://doi.org/10.1016/j.yfrne.2009.05.007>.
55. Ben-Ami Bartal, I., Breton, J.M., Sheng, H., Long, K.L., Chen, S., Halliday, A., Kenney, J.W., Wheeler, A.L., Frankland, P., Shilyansky, C., et al. (2021). Neural correlates of in-group bias for prosociality in rats. *eLife* 10, e65582. <https://doi.org/10.7554/eLife.65582>.
56. Song, D., Wang, C., Jin, Y., Deng, Y., Yan, Y., Wang, D., Zhu, Z., Ke, Z., Wang, Z., Wu, Y., et al. (2023). Mediodorsal thalamus-projecting anterior cingulate cortex neurons modulate helping behavior in mice. *Curr. Biol.* 33, 4330–4342.e5. <https://doi.org/10.1016/j.cub.2023.08.070>.
57. Zhang, M., Wu, Y.E., Jiang, M., and Hong, W. (2024). Cortical regulation of helping behaviour towards others in pain. *Nature* 626, 136–144. <https://doi.org/10.1038/s41586-023-06973-x>.
58. Chaibi, I., Bennis, M., and Ba-M'Hamed, S. (2021). GABA-A receptor signaling in the anterior cingulate cortex modulates aggression and anxiety-related behaviors in socially isolated mice. *Brain Res.* 1762, 147440. <https://doi.org/10.1016/j.brainres.2021.147440>.
59. Kim, J., Wasserman, E.A., Castro, L., and Freeman, J.H. (2016). Anterior cingulate cortex inactivation impairs rodent visual selective attention and prospective memory. *Behav. Neurosci.* 130, 75–90. <https://doi.org/10.1037/bne0000117>.
60. Totah, N.K.B., Kim, Y.B., Homayoun, H., and Moghaddam, B. (2009). Anterior cingulate neurons represent errors and preparatory attention within the same behavioral sequence. *J. Neurosci.* 29, 6418–6426. <https://doi.org/10.1523/JNEUROSCI.1142-09.2009>.
61. Çavdaroğlu, B., and Balci, F. (2016). Mice can count and optimize count-based decisions. *Psychon. Bull. Rev.* 23, 871–876. <https://doi.org/10.3758/s13423-015-0957-6>.
62. Gür, E., Duyan, Y.A., and Balci, F. (2021). Numerical averaging in mice. *Anim. Cogn.* 24, 497–510. <https://doi.org/10.1007/s10071-020-01444-6>.
63. Borland, J.M., Walton, J.C., Norvelle, A., Grantham, K.N., Aiani, L.M., Larkin, T.E., McCann, K.E., and Albers, H.E. (2020). Social experience and sex-dependent regulation of aggression in the lateral septum by extrasynaptic α GABAA receptors. *Psychopharmacol. (Berl.)* 237, 329–344. <https://doi.org/10.1007/s00213-019-05368-z>.
64. Bredewold, R., Washington, C., and Veenema, A.H. (2023). Vasopressin regulates social play behavior in sex-specific ways through glutamate modulation in the lateral septum. Preprint at bioRxiv. <https://doi.org/10.1101/2023.03.31.535148>.
65. Wacker, D.W., Engelmann, M., Tobin, V.A., Meddle, S.L., and Ludwig, M. (2011). Vasopressin and social odor processing in the olfactory bulb and anterior olfactory nucleus. *Ann. N. Y. Acad. Sci.* 1220, 106–116. <https://doi.org/10.1111/j.1749-6632.2010.05885.x>.
66. Rodriguez, L.A., Kim, S.H., Page, S.C., Nguyen, C.V., Pattie, E.A., Hallock, H.L., Valerino, J., Maynard, K.R., Jaffe, A.E., and Martinowich, K. (2023). The basolateral amygdala to lateral septum circuit is critical for regulating social novelty in mice. *Neuropsychopharmacology* 48, 529–539. <https://doi.org/10.1038/s41386-022-01487-y>.
67. Kanyile, S.N., Pillay, N., and Schradin, C. (2021). Bachelor groups form due to individual choices or environmental disrupters in African striped mice. *Anim. Behav.* 182, 135–143. <https://doi.org/10.1016/j.anbehav.2021.10.005>.
68. Bai, F., Huang, L., Deng, J., Long, Z., Hao, X., Chen, P., Wu, G., Wen, H., Deng, Q., Bao, X., et al. (2023). Prelimbic area to lateral hypothalamus circuit drives social aggression. *iScience* 26, 107718. <https://doi.org/10.1016/j.isci.2023.107718>.
69. Biro, L., Sipos, E., Bruzsik, B., Farkas, I., Zelena, D., Balazsfi, D., Toth, M., and Haller, J. (2018). Task division within the prefrontal cortex: distinct neuron populations selectively control different aspects of aggressive behavior via the hypothalamus. *J. Neurosci.* 38, 4065–4075. <https://doi.org/10.1523/JNEUROSCI.3234-17.2018>.
70. Padilla-Coreano, N., Batra, K., Patarino, M., Chen, Z., Rock, R.R., Zhang, R., Hausmann, S.B., Weddington, J.C., Patel, R., Zhang, Y.E., et al. (2022). Cortical ensembles orchestrate social competition via hypothalamic outputs. *Nature* 603, 667–671. <https://doi.org/10.1038/s41586-022-04507-5>.
71. Porter, R.H. (1976). Sex-differences in the agonistic behavior of spiny-mice (*Acomys cahirinus*). *Z. Tierpsychol.* 40, 100–108. <https://doi.org/10.1111/j.1439-0310.1976.tb00928.x>.
72. Krashes, M.J., Koda, S., Ye, C., Rogan, S.C., Adams, A.C., Cusher, D.S., Maratos-Flier, E., Roth, B.L., and Lowell, B.B. (2011). Rapid, reversible activation of AgRP neurons drives feeding behavior in mice. *J. Clin. Invest.* 121, 1424–1428. <https://doi.org/10.1172/JCI46229>.
73. Schindelin, J., Arganda-Carreras, I., Frise, E., Kaynig, V., Longair, M., Pietzsch, T., Preibisch, S., Rueden, C., Saalfeld, S., Schmid, B., et al. (2012). Fiji: an open-source platform for biological-image analysis. *Nat. Methods* 9, 676–682. <https://doi.org/10.1038/nmeth.2019>.
74. Stirling, D.R., Swain-Bowden, M.J., Lucas, A.M., Carpenter, A.E., Cimini, B.A., and Goodman, A. (2021). CellProfiler 4: improvements in speed, utility and usability. *BMC Bioinformatics* 22, 433. <https://doi.org/10.1186/s12859-021-04344-9>.
75. Friard, O., and Gamba, M. (2016). M. Boris: a free, versatile open-source event-logging software for video/audio coding and live observations. *Methods Ecol. Evol.* 7, 1325–1330. <https://doi.org/10.1111/2041-210X.12584>.
76. Leroy, F., Park, J., Asok, A., Brann, D.H., Meira, T., Boyle, L.M., Buss, E.W., Kandel, E.R., and Siegelbaum, S.A. (2018). A circuit from hippocampal CA2 to lateral septum disinhibits social aggression. *Nature* 564, 213–218. <https://doi.org/10.1038/s41586-018-0772-0>.
77. Wright, E.C., Luo, P.X., Zakharenkov, H.C., Serna Godoy, A., Lake, A.A., Prince, Z.D., Sekar, S., Culkun, H.I., Ramirez, A.V., Dwyer, T., et al. (2023). Sexual differentiation of neural mechanisms of stress sensitivity during puberty. *Proc. Natl. Acad. Sci. USA* 120, e2306475120. <https://doi.org/10.1073/pnas.2306475120>.
78. Sharp, F.R., Sagar, S.M., Hicks, K., Lowenstein, D., and Hisanaga, K. (1991). c-fos mRNA, Fos, and Fos-related antigen induction by hypertonic saline and stress. *J. Neurosci.* 11, 2321–2331. <https://doi.org/10.1523/JNEUROSCI.11-08-02321.1991>.
79. Kelly, A.M., Fricker, B.A., and Wallace, K.J. (2022). Protocol for multiplex fluorescent immunohistochemistry in free-floating rodent brain tissues. *Star Protoc.* 3, 101672. <https://doi.org/10.1016/j.xpro.2022.101672>.
80. Carrillo, M., Han, Y., Migliorati, F., Liu, M., Gazzola, V., and Keysers, C. (2019). Emotional mirror neurons in the rat's anterior cingulate cortex. *Curr. Biol.* 29, 1301–1312.e6.
81. Oettl, L.-L., Ravi, N., Schneider, M., Scheller, M.F., Schneider, P., Mitre, M., da Silva Gouveia, M., Froemke, R.C., Chao, M.V., Young, W.S., et al. (2016). Oxytocin enhances social recognition by modulating cortical control of early olfactory processing. *Neuron* 90, 609–621. <https://doi.org/10.1016/j.neuron.2016.03.033>.
82. Yang, H., de Jong, J.W., Tak, Y., Peck, J., Bateup, H.S., and Lammel, S. (2018). Nucleus accumbens subnuclei regulate motivated behavior via direct inhibition and disinhibition of VTA dopamine subpopulations. *Neuron* 97, 434–449.e4. <https://doi.org/10.1016/j.neuron.2017.12.022>.
83. Yu, D., Xiao, R., Huang, J., Cai, Y., Bao, X., Jing, S., Du, Z., Yang, T., and Fan, X. (2019). Neonatal exposure to propofol affects interneuron development in the piriform cortex and causes neurobehavioral deficits in adult mice. *Psychopharmacol. (Berl.)* 236, 657–670. <https://doi.org/10.1007/s00213-018-5092-4>.
84. Xu, X., Zhou, H., Wu, H., Miao, Z., Wan, B., Ren, H., Ge, W., Wang, G., and Xu, X. (2023). Tet2 acts in the lateral habenula to regulate social preference in mice. *Cell Rep.* 42, 112695. <https://doi.org/10.1016/j.celrep.2023.112695>.

85. Okabe, S., Tsuneoka, Y., Takahashi, A., Ooyama, R., Watarai, A., Maeda, S., Honda, Y., Nagasawa, M., Mogi, K., Nishimori, K., et al. (2017). Pup exposure facilitates retrieving behavior via the oxytocin neural system in female mice. *Psychoneuroendocrinology* 79, 20–30. <https://doi.org/10.1016/j.psyneuen.2017.01.036>.
86. Kelly, A.M., and Seifert, A.W. (2021). Distribution of vasopressin and oxytocin neurons in the basal forebrain and midbrain of spiny mice (*Acomys cahirinus*). *Neuroscience* 468, 16–28. <https://doi.org/10.1016/j.neuroscience.2021.05.034>.
87. Dölen, G., Darvishzadeh, A., Huang, K.W., and Malenka, R.C. (2013). Social reward requires coordinated activity of nucleus accumbens oxytocin and serotonin. *Nature* 507, 179–184. <https://doi.org/10.1038/nature12518>.
88. Dumais, K.M., and Veenema, A.H. (2016). Vasopressin and oxytocin receptor systems in the brain: sex differences and sex-specific regulation of social behavior. *Front. Neuroendocrinol.* 40, 1–23. <https://doi.org/10.1016/j.yfrne.2015.04.003>.
89. Grinevich, V., and Stoop, R. (2018). Interplay between oxytocin and sensory systems in the orchestration of socio-emotional behaviors. *Neuron* 99, 887–904. <https://doi.org/10.1016/j.neuron.2018.07.016>.
90. Robert, V., Therreau, L., Chevalyere, V., Lepicard, E., Viollet, C., Cognet, J., Huang, A.J., Boehringer, R., Polygalov, D., McHugh, T.J., et al. (2021). Local circuit allowing hypothalamic control of hippocampal area CA2 activity and consequences for CA1. *eLife* 10, e63352. <https://doi.org/10.7554/eLife.63352>.
91. Thirtamara Rajamani, K., Barbier, M., Lefevre, A., Niblo, K., Cordero, N., Netser, S., Grinevich, V., Wagner, S., and Harony-Nicolas, H. (2023). Oxytocin activity in the paraventricular and supramammillary nuclei of the hypothalamus is essential for social recognition memory in rats. Preprint at bioRxiv. <https://doi.org/10.1101/2022.05.23.493099>.
92. Paxinos, G., and Franklin, K. (2001). *The Mouse Brain in Stereotaxic Coordinates* (Academic Press).

STAR★METHODS

KEY RESOURCES TABLE

REAGENT or RESOURCE	SOURCE	IDENTIFIER
Antibodies		
Rabbit anti-c-Fos	Synaptic Systems	Cat# 226003; RRID: AB_2231974; lot 5-69
Bacterial and virus strains		
AAV8.pAAV-hSyn-DIO-hM4D(Gi)-mCherry	Krashes et al. ⁷²	Addgene; cat# 44362-AAV8; RRID: Addgene_44362
AAV8.pAAV-hSyn-mCherry	Karl Deisseroth	Addgene; cat# 114472-AAV8; RRID: Addgene_114472
retroAAV.pENN. AAV.hSyn.HI.eGFP-Cre.WPRE.SV40	James M. Wilson	Addgene; cat# 105540-AAVrg; RRID: Addgene_105540
Chemicals, peptides, and recombinant proteins		
Clozapine N-oxide (CNO) dihydrochloride (water soluble)	Hello Bio	Cat# HB6149
Invitrogen Dextran, Tetramethylrhodamine, 10,000 MW, Neutral	Thermo Fisher Scientific	Cat# D1816
Red Retrobeads	Lumafluor	https://lumafluor.com/shop/ols/products/xnred-retrobeads-100-l-o9a1330r
Software and algorithms		
GraphPad Prism	GraphPad	RRID: SCR_002798
FIJI	Schindelin et al. ⁷³	RRID: SCR_002285
Cell Profiler	Stirling et al. ⁷⁴	https://cellprofiler.org/ ; RRID: SCR_007358
SPSS 29	IBM	RRID: SCR_002865
Behavioral Observation Research Interactive Software (BORIS) project	Friard and Gamba ⁷⁵	https://www.boris.unito.it/ ; RRID: SCR_021434
Ethovision XT 17	Noldus	RRID: SCR_000441

EXPERIMENTAL MODEL AND STUDY PARTICIPANT DETAILS

Spiny mouse, *Acomys dimidiatus* (formerly known as *Acomys cahirinus*)

70 male and 64 female spiny mice (post-natal day (PND) 106–496, only 3 animals were older than 380 days, median age was PND 186) were used for behavioral testing, immunohistochemistry (IHC), and viral validation. 12 female C57BL/6J mice (Jax Strain number: 000664) purchased from The Jackson Laboratory (Bar Harbor, Maine) were used for a group size preference test. Subject sex was assigned based on external sexual organs, and littermates of the same sex were randomly assigned to experimental conditions. All procedures were approved by the Institutional Animal Care and Use Committee of Emory University (PROTO201900126). All methods were conducted in accordance with relevant ARRIVE guidelines and regulations. All methods were performed in accordance with the relevant guidelines and regulations. All animals were obtained from our breeding colony; breeders were from the captive-bred colony of Dr. Ashley W. Seifert (University of Kentucky). All animals were group-housed (2–4) in a standard rat polycarbonate cage (40.64 × 20.32 × 20.32 cm) lined with Sani-Chips bedding. Animals were provided with nesting material, rodent igloos, and shepherd shacks and were able to obtain food and water *ad libitum*. Spiny mice were kept on a 14-h light: 10-h dark cycle with an ambient temperature of 24 ± 2 °C.

METHOD DETAILS

Stereotaxic injections

Retrograde and anterograde tracing was achieved via two 350nL intracranial injections into the LS (coordinates: 2.3mm anterior, 0.44mm lateral, depths 3.2 and 2.8mm) into a single hemisphere. The injection consisted of a 1:1 mixture of undiluted Green Dextran, Tetramethylrhodamine, 10,000 MW (Invitrogen) and Lumafluor Red Retrobeads that had been diluted 1:1 with sterile saline. For chemogenetic experiments, conditional expression of hM4Di gene was achieved by two 200nL injections of retrograde AAV cre

(retroAAV.pENN.AAV.hSyn.HI.eGFP-Cre.WPRE.SV40, titer: 2.6×10^{13} Gc/mL) into the LS (Coordinates: 2.20mm anterior, 0.44mm lateral, depths 3.3 and 3.2mm) and encoding a double-floxed inverted open reading frame (DIO) of the hM4Di gene. The hM4Di AVV (AAV8-pAAV-hSyn-DIO-hM4D(Gi)-mCherry, titer: 2.2×10^{13} Gc/mL) or mCherry serotype (AAV8-pAAV-hSyn-mCherry, titer: 2.6×10^{13} Gc/mL) were intracranially injected twice at volumes of 150nL into the ACC (coordinates: 2.30mm anterior, 0.6mm lateral, depths 2.1 and 1.9mm).

For all intracranial injections, subject spiny mice received a 1.5mg/kg dose of meloxicam orally 30 minutes prior to anesthetization with isoflurane (4% for induction, 2% for maintenance). Subjects were placed into a stereotaxic setup (Kopf), and all AAVs were delivered through a pulled glass pipette at a rate of 1nl/sec using a nanosyringe (Drummond Nanoject III). Pipettes were held at the lowest injection site for 5 min and the final injection site for 10 min following AAV release. Coordinates were slightly adjusted based on mouse age and size, and viral vectors were allowed to express for 1 week for tracing injections and at least 5 weeks for chemogenetic injections before behavioral testing. During this time, all subjects were group-housed with up to 3 other same-sex littermates.

Validation of cre-dependent inhibitory DREADDs in spiny mice

To confirm that activation of cre-dependent inhibitory designer receptors exclusively activated by designer drugs (DREADDs) within the ACC decreases neural activity, we first ran an initial between-subjects validation study in eight male spiny mice. Half of the subjects received a uni-lateral intracranial injection of cre AAVs into the LS and an injection of the cre-dependent DREADD Dio-hM4Di into the ACC, ensuring that only ACC neurons that project to the LS will express DREADDs. The other half of subjects received the same cre injection within the LS and an mCherry AAV into the ACC (Figures S4A, S4D, and S4E), serving as a viral control group. After five weeks of incubation, all subjects received an intraperitoneal (IP) injection of 10mg/kg Clozapine N-oxide (CNO) 30 min prior to a 30 min social interaction test with a novel, same-sex conspecific. This social interaction was followed by an additional 30 min of isolation and then perfusion to capture Fos responses to exposure to the novel, same-sex conspecific 1 hr after CNO had 30 min to begin affecting the brain. Exposure to a single, same-sex conspecific was chosen for validation because the tracing IEG study above demonstrated that such a social exposure sufficiently induces activity in LS-projecting ACC neurons. Brain tissue from each subject underwent IHC to visualize colocalization of Fos-ir with Dio-hM4Di or mCherry cell body expression (Figure S4B). Analysis revealed a significant difference between groups ($t_{(22)} = 6.617$, $p < 0.001$) such that the Dio-hM4Di condition ($M = 23.352$) had a significantly lower percentage of colocalized neurons than the mCherry condition ($M = 83.305$; $MD = 58.953$), confirming for the first time the efficacy of cre-dependent inhibitory DREADDs in spiny mice (Figure S4C).

Behavioral Assays

Immediate Early Gene (IEG) studies

For logistical reasons related to work restrictions induced by the pandemic, our initial IEG studies were conducted on a 60 min timeline, which has been previously used to identify cellular responses to stimulus exposure.^{21,76,77} For consistency throughout the project, a 60 min timeline was used for all IEG studies.

Social vs. Nonsocial IEG. To confirm that the LS is responsive to social stimuli, four male and four female spiny mice were exposed to either a novel, same-sex conspecific or a novel rubber duck. Subjects were transferred to a clean, standard rat polycarbonate cage (40.64 x 20.32 x 20.32 cm), followed by either a conspecific stimulus animal or a rubber duck. Subjects were allowed to interact with the stimuli for 30 min. The stimuli were then removed from the test cage and the subject remained in the cage for an additional 30 min prior to undergoing a perfusion to capture Fos-ir+ expression in response to the stimulus exposure.

Small vs. Large Group Exposure IEG. We ran two identical IEG studies to first identify an initial region within the rodent social brain network (SBN) that differentially responds to peer group size in 12 male and 14 female spiny mice (note that males and females were tested at different dates and thus were not analyzed in the same model), and then determine upstream and downstream regions from the LS also differentially respond to peer group size in 12 male and 12 female spiny mice. For both IEG studies, all subjects were placed in a large Plexiglas testing chamber (60.96 x 45.72 x 38.1 cm) with either a single, novel, same-sex conspecific or a group of 7 novel, same-sex conspecifics confined under their own wire mesh container in the center of the testing chamber. Subjects were allowed to investigate the stimulus animals for 30 min before being transferred to a clean, standard rat polycarbonate cage (40.64 x 20.32 x 20.32 cm) for an additional 30 min prior to undergoing a perfusion to capture Fos-ir+ expression in response to the stimulus exposure. All interactions were recorded. For the second IEG to examine upstream and downstream regions of the LS, all subjects received their cranial injections 1 week prior to the IEG.

c-fos mRNA can be detected as early as 5 min after exposure to a stimulus and peaks at 30-60 min, whereas Fos protein is maximal at 1-2 hr.⁷⁸ Although 60-90 min timelines are traditionally used for IEG studies examining Fos responses, it is possible that our IEG studies may have captured some very early Fos responses at the 30 min timepoint when stimuli were removed from test cages prior to perfusion. Thus, there is the potential that our results may contain neural responses to the stimuli being removed from test cages; notably, this would be consistent across all treatment groups/exposure types since all subjects had stimuli removed 30 min after exposure and 30 min prior to perfusion.

Group size preference tests

We developed a new group size preference test chamber based on our previous behavioral test¹⁵ for use in the social peer group size preference test and the nonsocial group size preference test. The testing chamber consists of an initial acrylic chamber (15.24 x 15.24 x 45.72 cm) that releases subjects into a large, opaque acrylic chamber (55.88 x 71.12 x 45.72 cm) divided into two identical sections.

Each section can hold up to 8 stimulus animals or objects, separated from the subject by clear acrylic with 0.12 cm diameter holes. When the subject is in one section, their view of the other section is entirely obstructed (Figure 3B).

The order of social and nonsocial group size preference tests was counterbalanced across subjects. Subjects were given an intraperitoneal (IP) injection of either saline or 10mg/kg of CNO 30 minutes prior to testing. Subjects were then released from the initial holding chamber into the larger chamber and allowed to affiliate with and investigate both sides of the chamber, one side of which contained a small (2) group and the other side a large (8) group of novel, same-sex conspecifics for the social peer group size preference test or a small (2) and large (8) group of novel, spiny mouse-sized rubber ducks for the nonsocial group size preference test. The location of the small and large groups were counterbalanced. After 20 min, the subjects were removed from the chamber and returned to their home cage. Roughly 1 hr later, subjects were tested again for group size preference (social or nonsocial, depending on test type for the first test).

The first 10 min of each test were hand scored by a single observer, blind to experimental treatment, using BORIS.⁷⁵ We quantified the amount of time each subject spent near each group and investigating each group. The chamber was divided into four quadrants, where the quadrants closest to each group were considered “near” the group, and investigation was considered as pressing one’s nose up to a chamber containing a stimulus animal. Using these values, we calculated three behavioral scores: (1) an affiliation score, which was a normalized score based on the time near the large group minus the small group, (2) an investigation score, which was a normalized score based on the time spent investigating the large group minus the small group, and (3) an antisocial score, which was the percentage of the test time that the subject spent in one of the two quadrants not near either group. Additionally, the velocity of each animal during the behavioral tests were obtained with automated tracking via Ethovision XT 17 (Noldus, Leesburg, VA, USA).

Histology and immunohistochemistry

All histology and immunohistochemistry followed our previously published protocol.⁷⁹ For both IEG studies, subjects were immediately euthanized at the end of the test by isoflurane overdose and were transcardially perfused with 0.1 M phosphate buffer saline (PBS) followed by 4% paraformaldehyde. Brains were extracted, post-fixed overnight in 4% paraformaldehyde, and underwent cryoprotection in 30% sucrose dissolved in PBS for 48 h. Brains were frozen in tissue-tek O.C.T. compound and stored at -80 °C before sectioning coronally at 40 for the first or 30 μ m (due to the retrobead protocol) for the second IEG using a Leica cryostat, with every third section saved for use in the present study. Tissue sections were immunofluorescently stained for Fos (the protein of the immediate early gene cFos; Synaptic Systems rabbit c-Fos 1:1000 dilution).

For targeting confirmation of the chemogenetic experimental animals, transcardial perfusions, post-fixing, and sectioning occurred identically to how the IEG study brains were processed. However, no immunofluorescent staining took place. Instead, sectioned tissue was mounted directly onto slides after rinsing in PBS.

Neural Quantification

Photomicrographs were obtained using a Zeiss AxioImager II microscope fitted with an apotome. For all regions quantified, we took 10 \times images and quantified the average number of Fos-ir+ and retrobead labeled (when appropriate) cells and the number of cells that co-expressed retrobeads and Fos across 3 consecutive tissue sections that spanned the rostral-to-caudal axis. This totaled 120 or 90 μ m for the first and second IEG respectively, and the initial anterior-posterior coordinates from bregma are reported in Tables S1–S3. Due to differences in retrobead staining across consecutive sections, the percent retrobead labeled neurons that were Fos-ir+ measure was analyzed for each individual section as well as the average across all three, while the Fos-ir+ measure was analyzed for the average across sections. FIJI⁷³ was used to create standard regions of interest (ROIs) for all regions, and a Cell Profiler⁷⁴ pipeline was created to automatically count fluorescent cells and nuclei and to identify colocalized neurons. For retrograde tracing analysis, the Fos-retrobead colocalization was calculated separately due to differences in retrobead abundance from rostral to caudal portions of each region. For all other analyses, however, the Fos-ir values across all sections were averaged together.

Brain regions analyzed for retrobead labeling included: the anterior cingulate cortex (ACC; implicated in consolation behavior and contains emotional mirror neurons^{36,80}), the anterior olfactory nucleus (AON; critical for social recognition⁸¹ and social odor cue processing⁶⁵), the basolateral amygdala (BLA; responds to social novelty⁶⁶), the ventral tegmental (VTA; regulates reward⁸² and aggression³⁷) and the piriform cortex (PC; involved in processing of social odor cues⁸³).

Brain regions analyzed for anterograde labeling included: the lateral hypothalamus (LH; involved in aggression and social dominance^{29,70}), the lateral habenula (LHb; facilitates social preferences⁸⁴), the lateral preoptic nucleus (IPOA; responds to pup retrieval and parenting behavior⁸⁵), the median preoptic nucleus (MnPO; shown to have oxytocin producing neurons in spiny mice⁸⁶), the mPOA (crucial for parental care^{43,44}), the nucleus accumbens (NAc; promotes social reward⁸⁷), the paraventricular nucleus of the hypothalamus (PVN; major source of oxytocin and vasopressin within mammals^{88,89}), and the supramammillary nucleus (SuM; influences social recognition and social memory^{90,91}).

For tracing studies, subjects were included in the analysis if the injection site was less than 90 μ m anterior to the merged anterior commissure (2.3mm anterior to bregma) and between 1.5 and 3.25mm from the top of the cortex. For chemogenetic studies, subjects were included in the analysis if the cre injection was less than 120 μ m anterior to the merged anterior commissure (2.3mm anterior to bregma) and between 1.5 and 3.25mm from the top of the cortex. Additionally, the hM4Di/mCherry injection site was required to be between 1.38 and 2.3mm from bregma and not fall below the corpus collosum. All figure schematics displaying injection locations are adapted from Paxinos The Mouse Brain in Stereotaxic Coordinates.⁹²

QUANTIFICATION AND STATISTICAL ANALYSIS

Behavioral measurements for each test were analyzed using SPSS 29 (IBM Analytics). Tests used include independent t-tests when comparing two means for experiments detailed in [Figures 1, S2, S4, S7, and S8](#). General linear models (GLM) that include Exposure Type and Sex as fixed factors were used for experiments detailed in [Figures 2, 5, S1, S3, S6, and S9](#). GLMs with Condition and Sex as fixed factors were used for experiments detailed in [Figures 3 and 4](#). To correct for multiple comparisons, all *post-hoc* pairwise comparisons were adjusted using Sidak corrections. The tests used for specific analyses are detailed in the figure legends. We screened for outliers for each individual test, defined as 3 standard deviations outside the mean, but none were found.